J Mater Sci (2007) 42:9234–9238
DOI 10.1007/s10853-007-1897-y

Size influence on optical absorption property of ultra-fine nickel hollow spheres

Zhibin Li · Yida Deng · Yating Wu · Bin Shen · Wenbin Hu

Received: 28 March 2007 / Accepted: 29 May 2007 / Published online: 27 July 2007

Abstract Nickel hollow spheres (NHSs) with different diameter have been synthesized by the autocatalytic reduction method. The morphology, particle size distribution and optical absorption property of NHSs were investigated. The optical absorption intensity obviously increases in ultraviolet—near infrared region with the decrease of particle size. While in infrared region, nickel hollow spheres have almost no absorption. After the heat treatment process, the grain sizes of samples become bigger and the absorptances decrease in UV–Vis–NIR region. For smaller particles, the absorption peak in ultraviolet range moves from 375 to 440 nm because of the increase of grain size after heat treatment.

Introduction

Ultra-fine hollow spheres have been extensively studied in recent years. These hollow particles exhibit novel properties (for example, low density, large specific surface area, good permeability, and interesting optical properties), which make them attractive from both scientific and technological viewpoints. Potential applications for such hollow particles are artificial cells, catalysts, protection of biologically active agents, delivery of drugs, cosmetics, inks and dyes [1–7]. Among the methods used to fabricate hollow spheres, the template-synthetic route is often employed. To date, the templates used mainly include polystyrene sphere [8–10], resin sphere [2], micelles [11–13], microemulsion droplets [14–17], silica colloid spheres [18], macromolecular micelles [19] and mixed micelles of macromolecules and surfactants [20].

Although various hollow spheres have been prepared, few reports about optical property of hollow sphere were found [21–23]. In this paper, nickel hollow spheres with different size were synthesized by the autocatalytic reduction method [24]. The morphologies, size distribution and optical absorption property of the NHSs were characterized. The influence of particle size on optical absorption property of the NHSs was discussed.

Z. Li · Y. Deng · Y. Wu · B. Shen · W. Hu (✉)
State Key Laboratory of Metal Matrix Composites, Shanghai Jiao Tong University, Shanghai 200030, P.R. China
e-mail: material_hu@163.com

Experimental

Preparation

Based on the previous work of our group [25], NHSs were prepared by means of autocatalytic reduction method. During the preparation process, analytically pure $NiSO_4 \cdot 6H_2O$, $NaH_2PO_2 \cdot H_2O$, NaOH, acetic acid and citric acid as starting materials were used. Firstly, 20 g nickel sulfate, 0.1 g acetic acid and 0.15 g citric acid were dissolved in de-ionized water to get 200 mL Ni^{2+} mixture solution. About 3 g sodium hydroxide and 25 g sodium hypophosphite were dissolved in 200 mL de-ionized water in beakers, respectively. All solutions were preheated at 80 °C for 5 min. Then the Ni^{2+} solution and alkali solution were mixed by violent stirring, followed by producing a viridescent colloid. And then the sodium hypophosphite solution was added to the as-prepared colloid by evenly stirring. Finally, one dark-gray powder was obtained after the reaction had taken place for 5 min, and the powder was repeatedly washed with ammonia

and de-ionized water. The final products were dried in vacuum furnace at 100 °C for 2 min. By increasing the quantity of sodium hydroxide from 3 g to 6 g with the step of 1 g, four samples (sample A–D) with different size were prepared.

Characterization

The morphologies of hollow spheres were characterized through field emission scanning electron microscope (FE-SEM) with FEI SIRION 200 microscope, operated at acceleration voltage of 5.0 kV. The samples were coated gold by sputtering for 5 min at 1.5 mA. Transmission electron microscopy (TEM) images were recorded on a Philips CM200FEG microscope operating at 50 kV. X-ray powder diffraction (XRD) patterns of the samples were obtained on a D/max 2550V X-ray diffractometer using Cu Kα radiation at 40 kV and 100 mA. A Zetasizer Nano S photon correlation spectroscopy (PCS) nanoparticle size analyzer and a CIS-100 particle size & shape analyzer were used to estimate the particle size distributions of samples. Optical absorption properties of Ni hollow spheres were measured with a Cary 500 ultraviolet–visible–near infrared (UV-Vis-NIR) spectrophotometer at the wavelength range of 250–2500 nm and a EQUINOX 55 Fourier transform infrared-Raman (FTIR) spectroscope at the wavelength range of 2.5–25 μm.

Results and discussion

Morphology and structure

The morphologies of NHSs are shown in Fig. 1. It is observed that all the samples exhibit spherical morphology. The hollow structure of samples can be seen in inserted images of (A) and (B). Diameter of NHS sharply decreases with the increase of NaOH concentration. Diameters of sample A, B, C and D are about 2 μm, 700 nm, 200 nm and 70 nm, respectively. However sample C and D have homogeneous particle size distribution compared with sample A and B.

Particle size distribution of sample A was determined with particle size & shape analyzer and other samples were measured with PCS nanoparticle size analyzer. As shown in Fig. 2, the average diameters of samples from A to D are 2157.82, 950.48, 224.80, 98.90 nm respectively, consisting with the particle size shown in Fig. 1.

XRD patterns of NHSs are shown in Fig. 3. The diffraction peaks in the range of $20 < 2\theta < 80°$ can be indexed as face-centered cubic (fcc) Ni (111), (200) and (220), which indicate that the nickel spheres are polycrystalline. The peaks are fairly broad, even overlapping with neighbors, indicating the small grain size. This phenomenon becomes more obvious as particle size decreases. A rough estimation employing Scherrer's equation indicates the grain sizes of different sample from A to D are 6.2, 4.9, 2.1 and 1.5 nm respectively.

Optical absorption properties

Optical absorption of samples with different diameter at UV–Vis–NIR region was measured by using spectrophotometer. In Fig. 4, the absorptance of samples obviously increases in UV–Vis–NIR region with the decrease of diameter. It can be explained that the number of particles in unit volume increases when particle size become smaller, which improves multiscattering absorption. Additionally, surface effect and small size effect are more important reasons enhancing the absorption of samples.

In ultraviolet region, the absorptances of sample A and B decrease with the increase of wavelength, which are different from that of sample C and D. An absorption peak appears at 375 nm for sample C and D, which may be caused by small size effect of nano-particles. Some noble metallic nano-particles (Au, Ag) showed a plasma-resonance absorption in UV–Vis region [26, 27]. Although particle size of sample C and D are far bigger than that of nano-particles reported in literatures, the thickness of shell are nano-scale. So the peak at 375 nm may be due to the surface plasmon resonance absorption.

In visible region, the absorptance of samples decreases as wavelength increases. But sample A and B have different character from sample C and D. As wavelength increases in visible region, the absorptance of the former decreases more quickly than that of the latter. In near infrared region, absorptions of all samples are obviously weaker than that in UV-Vis region. Three peaks at 1385 nm, 2049 nm and 2213 nm may be caused by vibration of P–Ni bond.

In infrared region, optical transmission of samples was studied with FTIR spectroscope. As shown in Fig. 5, the transmittances of samples increase with wavelength increasing. At about 3,440 and 1,630 cm^{-1}, there are two absorption peaks that are attributed to bending vibration and stretching vibration of O–H. It could be explained that, inside the hollow sphere, there are residual substances including $Ni(OH)_2$, PO_2 or H_2O. And more residual materials may be contained in NHSs with smaller diameter because of fast reaction in preparation process [24], which cause some absorption peaks. According to IR-transmission spectra of samples, it can be concluded that nickel hollow spheres have almost no absorption of infrared light.

Effect of heat treatment

In addition, all samples were kept in furnace in hydrogen atmosphere at 250 °C for 1 h. In order to distinguish from

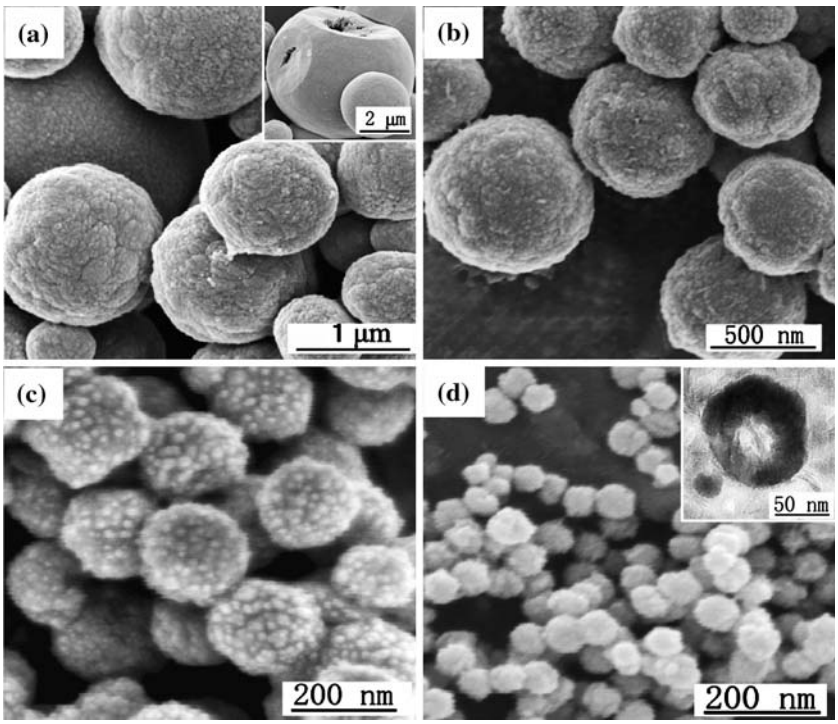

Fig. 1 FE-SEM micrographs of samples. A insert is a crushed sphere. D insert is the TEM image of a NHS

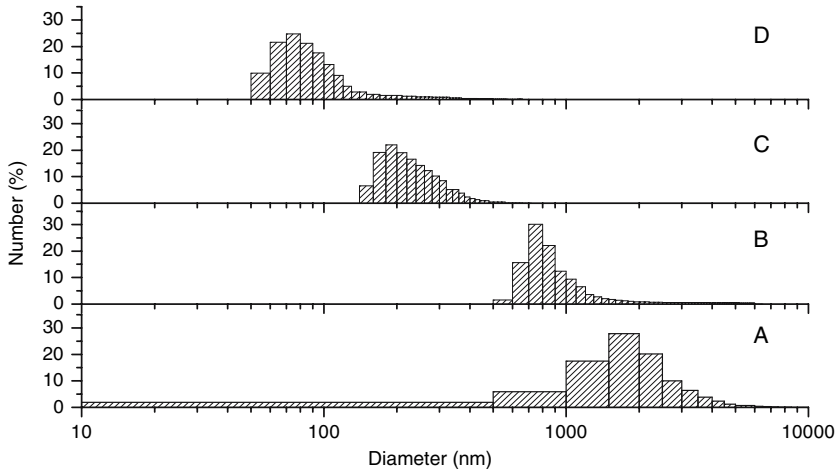

Fig. 2 Particle size distributions of samples

original samples, a suffix (TH) is added on the previous marker. After the heat treatment process, the grain sizes of samples become bigger. This can be proved by XRD patterns in Fig. 6. The peaks become clearer than those before heat treatment process and adjacent peaks are detached obviously. According to Scherrer's equation, the grain sizes of sample A, B, C and D are 10.5, 8.2, 6.8, 5.6 and 4.3 nm, respectively.

The optical absorption property of samples is affected by the heat treatment process, which can be seen in Figs. 7 and 8. In Fig. 7, the configuration of curves is similar to that in Fig. 4. But the absorptances of samples decrease appreciably after heat treatment process. For sample C and D, the absorption peak in ultraviolet region moves from 375 to 440 nm, which may be caused by the increase of grain size. The heat treatment and reduction of hydrogen also remove the residual $Ni(OH)_2$ and H_2O inside the NHSs, which reduce the absorption caused by bending vibration and stretching vibration of O–H (Fig. 8).

Conclusions

NHSs with different diameter have been synthesized by the autocatalytic reduction method. The morphologies, size distribution and optical absorption property of NHSs were characterized. The results indicate that when the hollow Ni spheres become smaller, the optical absorption

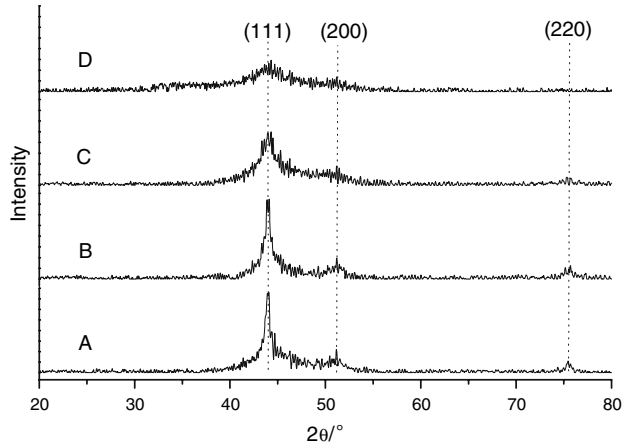

Fig. 3 XRD patterns of samples

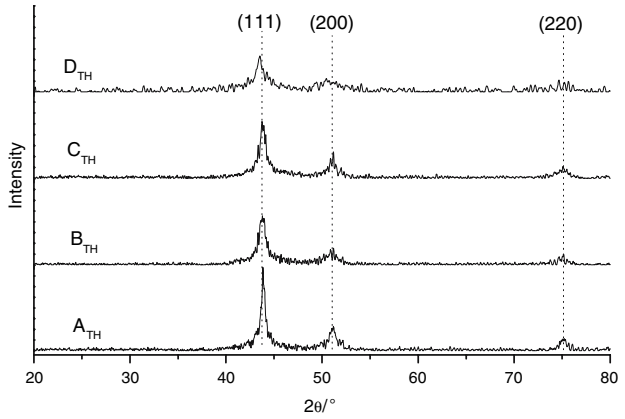

Fig. 6 XRD patterns of samples after heat treatments process

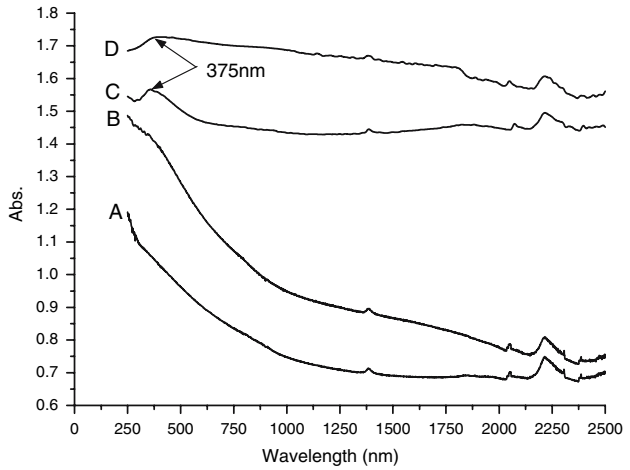

Fig. 4 UV–Vis–NIR absorption spectra of samples

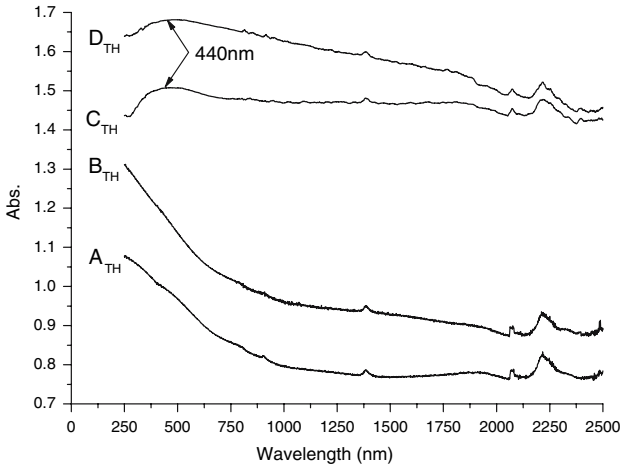

Fig. 7 UV–Vis–NIR absorption spectra of samples after heat treatment process

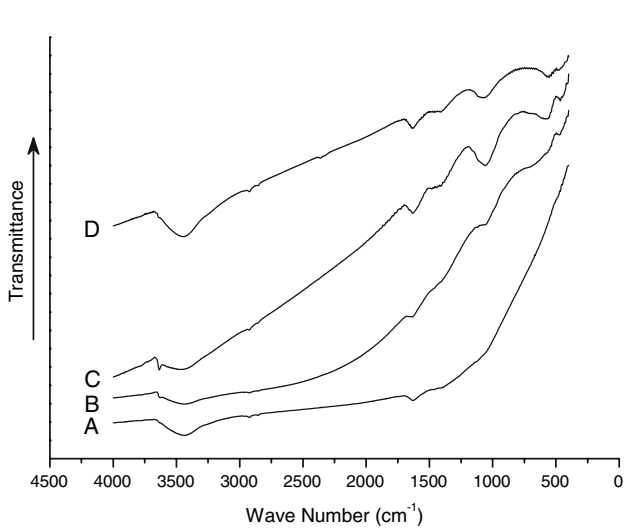

Fig. 5 IR-transmission spectra of samples

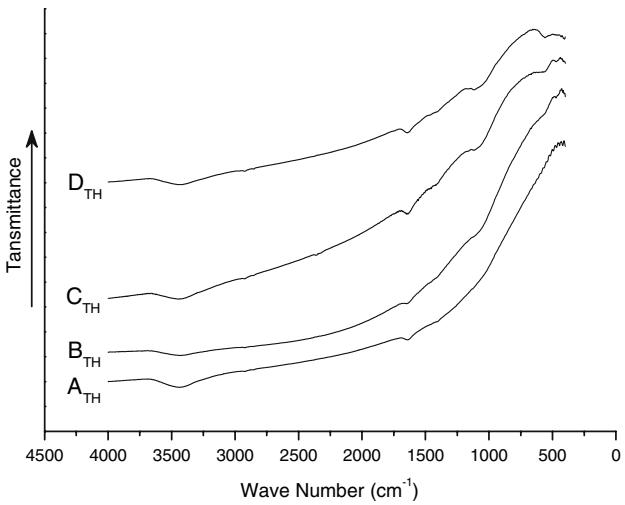

Fig. 8 IR-transmission spectra of samples after heat treatment process

intensity obviously increases in ultraviolet—near infrared region. While in infrared region, NHSs have almost no absorption. After the heat treatment process, the grain size of samples became bigger and the absorptances decrease in UV-Vis-NIR region. For smaller particles, the absorption peak in ultraviolet range moves from 375 to 440 nm because of the increase of grain size after heat treatment.

Acknowledgements This work is supported by National Natural Science Foundation of China (Grant no. 50474004), Shanghai Science and Technology committee Nano Special Fund (Grant no. 0552nm004), the "Dawn" Program of Shanghai Education Commission and the New-Century Training Program Foundation for Talents from the Ministry of Education of China.

References

1. Mathlowitz E, Jacob JS et al (1997) Nature 386:410
2. Bourlinos AB, Karakassides MA, Petridis D, Petridis D (2001) Chem Commun 1518–1519
3. Yin YD, Lu Y, Gates B, Xia YN (2001) Chem Mater 13:1146
4. Gau H, Herminghaus S, Lenz P, Lipowsky R (1999) Science 283:46
5. Zhang D, Qi L, Ma J, Cheng H (2002) Adv Mater 14:1499
6. Kim SW, Kim M, Lee WY, Hyeon T (2002) J Am Chem Soc 124:7642
7. Huang H, Resen EE (1999) J Am Chem Soc 121:3805
8. Chen Z, Zhan P, Wang Z, Zhang J, Zhang W, Ming N, Chan CT, Sheng P (2004) Adv Mater 16:417
9. Caruso F, Shi X, Caruso RA, Susha A (2001) Adv Mater 13:740
10. Li GC, Zhang ZK (2004) Mater Lett 58:2768
11. Lootens D, Vautrin C, Van Damme H, Zemb T (2003) J Mater Chem 13:2072
12. Koh K, Ohno K, Tsujii Y, Fukuda T (2003) Angew Chem Int Ed 42:4194
13. Hentze HP, Raghavan SR, McKelvey CA, Kaler EW (2003) Langmuir 19:1069
14. Song LY, Ge XW, Wang MZ, Zhang ZC (2006) J Non-Cryst Solids 352:2230
15. Liu HJ, Ni YH, Wang F, Yin G, Hong JM, Ma Q, Xu Z (2004) Colloid Surface A 235:79
16. Bao JC, Liang YY, Xu Z, Si L (2003) Adv Mater 15:1832
17. Jiang YQ, Zhao JZ, Bala H, Xu HF, Tao NN, Ding XF, Wang ZC (2004) Mater Lett 58:2401
18. Zhang JH, Zhan P, Liu HY, Wang ZL, Ming NB (2006) Mater Lett 60:280
19. Liu T, Xie Y, Chu B (2000) Langmuir 16:9015
20. Qi L, Li J, Ma J (2002) Adv Mater 14:300
21. Song CX, Wang DB, Gu GH, Lin YS, Yang JY, Chen L, Fu X, Hu ZS (2004) J Colloid Interf Sci 272:340
22. Hu Y, Chen JF, Chen WM, Li XL (2004) Adv Mater 14:383
23. Xu LS, Chen XH, Wu YR, Chen CS (2006) Nanotechnology 17:1501
24. Deng YiDa, Zhao Ling, Liu Lei, Shen Bin, Hu Wenbin (2005) Mater Res Bull 40:1864
25. Deng Yida, Liu Xi et al (2006) J Magnet Magnet Mater 303:181
26. Ichiro T, Tsuneo M (1995) J Non-Crystal Solids 181:77
27. Matz W (1998) J Mater Sci 33:155